UKAEA-CCFE-PR(19)68

Mikhail Yu. Lavrentiev, Chu-Chun Fu, Frédéric Soisson

Correlation between microstructure and magnetic properties during phase separation in concentrated Fe-Cr alloys

Correlation between microstructure and magnetic properties during phase separation in concentrated Fe-Cr alloys

Mikhail Yu. Lavrentiev, Chu-Chun Fu, Frédéric Soisson

Correlation between microstructure and magnetic properties during phase separation in concentrated Fe-Cr alloys

Mikhail Yu. Lavrentiev[(1),*], Chu-Chun Fu[(2)], Frédéric Soisson[(2)]

[(1)]*United Kingdom Atomic Energy Authority, Culham Science Centre, Abingdon, Oxon, OX14 3DB, United Kingdom*

[(2)] *DEN-Service de Recherches de Métallurgie Physique, CEA, Université Paris-Saclay, F-91191 Gif-sur-Yvette, France*

[*]Corresponding Author, E-mail: Mikhail.Lavrentiev@ukaea.uk

Abstract

We report a theoretical study of microstructure, magnetic properties, and their relationship in relatively concentrated Fe-Cr alloys in both Fe- and Cr-rich regions. Annealing of initially random systems at 500° C for times of the order of 10^6 s substantially changes their microstructure. In both systems, solute atoms form clusters with their sizes increasing with time according to power law, with exponent being close to 0.2. For the Fe-32 at. % Cr alloy, magnetization and the Curie temperature increase with increasing annealing time and cluster size. At large simulation times, the Curie temperature approaches its value for Fe-15 at. % Cr, the concentration of completely phase-separated iron-rich alloy. For the Cr-25 at. % Fe alloy, precipitation also results in an increase of magnetization and the Curie temperature, although characteristic times are about one order of magnitude greater.

I. INTRODUCTION

Body-centered cubic (bcc) iron-chromium alloys are a basis for steels to be used in several technological fields, for instance in future fusion (ITER, DEMO) and generation IV fission nuclear reactors. As such, their properties are subject to many studies, both experimental and theoretical. Many of these studies are focused on dilute limits, that is, on Fe-Cr alloys in which one of the elements (usually Cr) has a small concentration, typically not exceeding 15-20 at. %. There are also many studies of decomposition and microstructure change in concentrated alloys, because Fe-Cr is a benchmark system to study spinodal decomposition (for experimental studies see e.g. [1-3]). Another area of microstructural studies in bcc alloys with high Cr or Fe content is the so called σ-phase that is thermodynamically stable at approximately equal atomic contents of Fe and Cr, and σ-α phase transition [4]. Magnetic studies of highly concentrated alloys were pioneered by Yamamoto [5] using Mössbauer spectroscopy for Fe-Cr alloys with Cr content between 20.1 and 46.5 wt. %. He annealed specimens at 500° C for 150 hours (5.4×10^5 s) and studied magnetization as a function of temperature afterwards. Recently, experimental investigation of phase decomposition in Fe-35 at. % Cr alloy using atom probe tomography as well as theoretical study by phase-field simulation, was performed by Yan *et al.* and Li *et al.* [6,7]. They found that the Cr-rich ά'-phase is interconnected in three-dimensional space after 500 hours (1.8×10^6 s) aging at temperatures between 700 and 750 K (i.e., very similar annealing conditions to those used by Yamamoto [5]) and estimated the time dependence of spinodal decomposition. The phase field model resulted in power law growth rate of the radius of ά-phase with time, the exponent being in the range 0.2-0.36 depending on the temperature and phase separation stage. However, all known to us theoretical studies of structural phase separation in highly concentrated Fe-Cr system do not take into account magnetic properties of concentrated Fe-Cr alloys. Simulation methods available to us allow to perform simultaneous structural and magnetic studies of such alloys which are important for an accurate understanding and prediction of the microstructural and magnetic evolution of the system. In this paper, we attempt to establish a correlation between magnetic and microstructural evolution of Fe-Cr alloys at relatively high concentrations of constituents. In particular, for the high-Cr alloy in Fe, we want to investigate whether the global magnetization and Curie point temperature T_C could be predicted from the properties of the two separating phases (α and ά), for instance how the characteristic size of the ά-phase precipitates is related to T_C. We perform theoretical

study of Cr alloy in Fe with concentration in high-Cr range (32 at. % Cr), as well as of Fe alloy in Cr with concentration in high-Fe range (25 at. % Fe). Both these concentrations correspond to the miscibility gap in thermodynamically equilibrated bcc Fe-Cr, away from the σ-phase. Also, for the case of Fe alloy in Cr, the concentration of Fe was chosen such that the system is magnetically still in the ferromagnetic-paramagnetic range. At even lower Fe concentration (10 to 20 at. %), the magnetic ground state of high-Cr Fe-Cr alloy is the spin glass [8,9], for which the methods used in this study are not suitable.

This paper is organized as follows. In Chapter II we introduce methods used in simulations. In Chapter III, the results of structural simulations and the simulations of magnetic properties of Fe-rich alloys are presented. Chapter IV deals with Cr-rich alloys evolution, and we discuss the results and conclude in Chapter V.

II. CALCULATION METHODS

The decomposition between the α and ά phases is first simulated with the diffusion model and the kinetic Monte Carlo (kMC) method developed by Senninger *et al.* [10]. Diffusion of iron and chromium atoms occurs by thermally activated jumps of vacancies towards first nearest neighbor (1nn) sites, with migration barriers computed by a broken-bond model. The free energy of each configuration is computed as a sum of pair interactions that depend on the local composition and on the temperature. The values of the pair interactions at 0 K were fitted to DFT calculations of alloy formation energies and vacancy migration barriers in various Fe-Cr configurations. The temperature dependence of pair interactions, which accounts for vibrational and magnetic entropic contributions, are mostly fitted to experimental data (the critical temperature of the α-ά miscibility gap and tracer and interdiffusion coefficients in Fe-Cr alloys) [11]. The models reproduce the original thermodynamic properties of the Fe-Cr alloys, with a change in the sign of the mixing energy around 10 at. % Cr and an asymmetrical miscibility gap at low temperatures [12]. It also reproduces the acceleration of the diffusion during the ferro- to paramagnetic transitions. This effect of the magnetic transition is nevertheless introduced in the diffusion model in a purely

phenomenological way. The model does not take explicitly into account the magnetic configuration, or the magnetization of the system.

Time evolution of the Fe-Cr alloys was simulated using kMC method. Simulation box consisted of 2^{21} = 2097152 (128×128×128) bcc unit cells and included single vacancy and 4194303 Fe and Cr atoms. The initial configuration of the system was chosen as a random mixture of Fe and Cr atoms. During the computational run, annealing at a constant temperature of 500° C for up to ~7.8×10^5 s for Fe-32 at. % Cr and up to ~2.2×10^6 s for Cr-25 at. % Fe, was simulated.

The magnetic properties of configurations obtained during the kMC simulations were calculated using Magnetic Cluster Expansion (MCE) method that was developed for Fe-Cr system [13] and successfully used to simulate its properties in a wide range of concentrations and temperatures, including bcc-fcc phase transition [14], Curie temperature as a function of Cr content [15], magnetic noncollinearity at Fe/Cr interfaces [16] and in Fe (Cr) nanoclusters in bulk Cr (Fe) [17]. This method requires more computational resources than the kMC simulation, and in order to use kMC results, configurations obtained in these runs were truncated. Only 524288 Fe and Cr atoms in ⅛ of the kMC simulation box (64×64×64 unit cells) were used as an input for MCE simulations. Magnetic properties such as magnetic moment and magnetic correlations were calculated in Monte Carlo runs. A Monte Carlo run consisted of equilibration and accumulation steps, each of them included 4000 attempts to change the vector of magnetic moment per atom. All simulations were fully noncollinear.

III. MICROSTRUCTURE AND MAGNETIC PROPERTIES OF FE-32 % CR ALLOY

The evolution of microstructure in Fe-32 at. % Cr with annealing time is shown in Figure 1. At 500°C, the phase diagram (Figure 2, modified from [10]) predicts phase separation between an α phase with a composition $x = 0.15$ and an α' phase with a composition $x = 0.852$. After 7.8×10^5 s, large clusters of chromium are formed in an initially random system. The evolution of distribution of chromium concentration in Fe is shown in Figure 3. A local concentration of Cr is computed on each bcc sites by measuring the surrounding atomic fraction of Cr atoms within a sphere ranging up to the fifth nearest neighbors (including 59

atoms). The distribution $f_{Cr}(x)$ of these local concentrations (i.e. the fraction of sites with a local Cr concentration x) makes it possible to follow the evolution of the composition and the proportion of the Cr-rich and Fe-rich phases. At $t = 0$, one observes one Gaussian peak at $x = 0.32$, corresponding to the initial homogeneous random solid solution. When the phase separation takes place, this peak shifts towards lower values, indicating a continuous decrease of Cr in the Fe-rich phase α (which finally reaches its equilibrium concentration $x_\alpha = 0.15$). At the same time a wide shoulder forms and grows at $x > 0.32$ corresponding to the formation of Cr-enriched regions, at long annealing times ($t > 9 \times 10^5$s) a distinct peak appears, centered at the composition of the α' phase. It is more difficult to follow the composition of the α' phase, due to its small volume fraction, but its composition approaches the equilibrium value $x_{\alpha'} = 0.852$. The structure factor $S(q)$ is the Fourier transform of the two-point correlations function of the system [18]. It can be directly measured by neutron small-angle neutron scattering [2]. The spherical average $S(q)$ displays a peak at low angles with a maximum at q_m. The intensity of peaks increases during the phase separation and q_m decreases. In Fe-32 at. % Cr (as well as in Cr-25 at. % Fe) alloys the solute concentration is high enough so that the minority phase does not form isolated precipitates, but a percolated or interconnected microstructure. The average distance between nearest branches of the minority domain can be estimated from the $S(q)$ dependence as π/q_m [2,19]. It is shown in Figure 4 as a function of time, increasing to about 4 nm at the end of simulation. The time dependence of π/q_m can be best fitted by a power function with the exponent close to 0.2:

$$\frac{\pi}{q_m} = 0.255 t^{0.1972} \tag{1}$$

with π/q_m in nm and time in s.

In order to study the change of magnetic properties of the system with the change of microstructure, we performed MCE simulations for the ten configurations obtained at times between 0.859 s and 783396 s. The magnetic moment per atom as a function of temperature and the magnetic moment relatively to its value at temperature $T = 1$ K are shown in Figure 5. The behavior of $M(T)/M(1\,K)$ (Figure 5b) is very different for initial stages of annealing and for long annealing times. This is in agreement with experimental results of Yamamoto [5], who also found difference in magnetization vs. temperature curves for quenched and annealed specimens. As the time increases, and Cr atoms form larger clusters, the Curie temperature of the alloy increases. In order to find the Curie temperature of transition from ferromagnetic to paramagnetic phase, T_C, the behavior of the magnetic moment as function of

temperature was fitted to the following function, which describes both low-temperature linear decrease of magnetization and its rapid fall at temperatures close to the magnetic transition:

$$M(T)/M(T = 1\ K) = (1 - aT)\frac{1+\exp(-\frac{b}{c})}{1+\exp(\frac{T-b}{c})} \qquad (2)$$

Then, T_C was estimated as the inflection point (temperature where the absolute value of derivative $\frac{\partial M}{\partial T}$ is maximal) of the fitted $M(T)$ curve and is shown in Figure 6a as a function of annealing time. It demonstrates characteristic sigmoid-type saturation behavior, approaching the Curie temperature of Fe-15 at. % Cr (~1020 K in the current MCE simulation) at long times. Dependence of the Curie temperature on π/q_m is shown in Figure 6b. Unlike the dependence on annealing time, it does not show initial slow growth, starting with linear $T_C(\pi/q_m)$ dependence, and moving to saturation regime at larger values of π/q_m. Linear dependence that can be approximated by the formula

$$T_C(K) = 657 + 170 \times \frac{\pi}{q_m}(nm) \qquad (3)$$

that describes the Curie temperature very well for values of π/q_m between 0.5 nm and 2 nm, corresponding to annealing times between 34 s and 21020 s at temperature 500° C.

IV. MICROSTRUCTURE AND MAGNETIC PROPERTIES OF CR-25 % Fe ALLOY

The evolution of microstructure in Cr-25 at. % Fe with time changing between 3 s and 2.3×10^6 s is shown in Figure 7. Again, as in case of Fe–32 at. % Cr, clear separation into two areas, Cr-rich, and Fe-rich, emerges with time. The evolution of distribution of Fe concentration is shown in Figure 8. The characteristic time necessary for the second maximum corresponding to high-concentration Fe clusters to emerge is higher in this case and of the order of 10^5-10^6 s. This is in agreement with slower vacancy-mediated diffusion in high-Cr alloys, related to higher vacancy-Cr migration barrier. For high-Fe alloys, DFT studies [20,21] predict value of 0.57 eV for vacancy-Fe exchange energy barrier and 0.64 eV for vacancy-Cr exchange barrier, and the two-band interatomic potential model [22] gives 0.56 eV for vacancy-Fe exchange barrier and 0.65 eV for vacancy-Cr exchange barrier. At the same time, vacancy-Cr exchange barrier in high-Cr alloys can exceed 1 eV [11]. The

value of π/q_m, calculated as in Section III, is shown in Figure 9 as a function of time. The π/q_m also increases to about 4 nm at the end of simulation and the time dependence of π/q_m can be best fitted by a power function with the exponent also very close to 0.2, i.e. to the one found for Cr clusters in Fe-rich system:

$$\frac{\pi}{q_m} = 0.2t^{0.2026} \tag{4}$$

Note that similar exponents close to 0.2 were already found in experiment [23,2] as well as in atomistic simulations [10].

Magnetic properties of configurations of Cr-25 at. % Fe with time changing between 3 s and 2.3×10^6 s were also studied in MCE simulations. The concentration of Fe in this system is rather high, so Cr subsystem does not demonstrate antiferromagnetic behaviour found in random Fe-Cr alloys at $x_{Fe} < 10$ at. % in our previous MCE simulations [21]. Experimental data also confirm that at concentrations above 20 at. % Fe, the alloy is in ferromagnetic phase with the Curie temperature close to 200 K at 25 at. % Fe ([24], Fig. 60). However, the Fe subsystem demonstrates clear ferromagnetism, with magnetic moment increasing with time, as Fe precipitates grow. Figure 10 shows magnetic moment per atom as function of time for several temperatures. Rapid increase of the moment begins at times of the order of 10^6 s, i.e. simultaneously with appearance of the second maximum on Fe concentration plot (Figure 8), indicating appearance of Fe precipitates. The behaviour of the magnetic moment as function of temperature is shown in Figure 11. In order to estimate the Curie transition temperature, we performed the same fit of magnetic moment as function of temperature (2) as in the case of Fe-32 at. % Cr. The results are plotted as functions of annealing time and the π/q_m in Figure 12. The time dependence of the T_C clearly demonstrates two regimes, almost flat up to times of the order of 10^5 s, and rapid rise after that. The Curie temperature in the first regime is between 200 and 300 K, which is in good agreement with available experimental data for quenched Fe-Cr alloys with similar concentration [24,25]. In the second regime, at times longer than 10^5 s, and with the π/q_m larger than 2 nm, the Curie temperature increases similarly to the case of Fe-32 at. % Cr. For the longest simulation times (over 10^6 s), the Curie temperature approaches values over 800 K. This is lower than ~1020 K as obtained for Fe-15 at. % Cr in the current MCE simulations, because (a) vacancy-mediated evolution is slower in Cr-rich alloys compared to Fe-rich, and (b) iron-rich minority phase in Cr-25 at. % Fe is affected by chromium-rich surroundings that suppress ferromagnetism.

V. DISCUSSION AND CONCLUSIONS

We have studied microstructure evolution and accompanying change in magnetic behavior of Fe-Cr alloys with high concentration of both components. First, change of microstructure under conditions of long-term annealing at 500° C starting from random alloys was studied. Growth of solute precipitates was observed in both Fe–32 at. % Cr and in Cr-25 at. % Fe. The time dependence of π/q_m can be described by power law with exponent very close to 0.2 for both Cr precipitates growth in Fe, and Fe precipitates in Cr. This time dependence is in a very good agreement with phase modelling results obtained recently by Yan *et al.* [6] who found this parameter in Fe-35 at. % Cr to change between 0.2 and 0.36 depending on annealing temperature and phase separation stage. Li *et al.* [7] performed similar study for alloys with Cr content between 25 and 35 at. % and found the exponent to be between 0.12 and 0.21 in growth and coarsening phase. Other studies [2,10,23] also found exponents close to 0.2. Initially, both alloys have a single maximum at a plot on concentration of the solute. With increasing annealing time, two clear maxima appear, one corresponding to single atoms and small clusters dissolved in large-concentration phase, and the other corresponding to emerging of relatively large solute precipitates with high solute concentration. The characteristic times necessary to form a two-maxima distribution are shorter for the Fe-32 at. % Cr alloy than for the Cr-25 at. % Fe alloy, which is related to slower vacancy-mediated diffusion in chromium compared to iron. Magnetic phase transition temperature increases with annealing time in both alloys studied. In Fe-32 at. % Cr alloy, it approaches Curie temperature of pure Fe. We found difference in the magnetization curves between the quenched and the annealed cases similar to that found by Yamamoto [5]. At that time, the origin of this observation was unclear, but now we can state that this difference stems from formation and growth of ά-precipitates and decrease of Cr content in α-phase matrix with annealing time. An important observation was a linear dependence between the π/q_m and the Curie temperature (3) in a wide range of sizes and annealing times.

Concluding, for the first time simultaneous study of microstructural evolution and magnetic properties of highly concentrated Fe-Cr alloys was performed. This work was initially motivated by experiments of Yamamoto [5], but the computational facilities and methods available today allowed us to move beyond this initial aim and look at interplay of magnetism and microstructure in more details. It is shown that the growth of precipitates of solute phase leads to change of magnetic properties of the system, with Curie temperature also increasing.

In particular, for Fe-32 at. % Cr it almost reaches value of Fe-15 at. % Cr, the concentration of completely phase-separated iron-rich alloy, at longest simulation times.

References

1. M. Furusaka, Y. Ishikawa, and M. Mera, *Phys. Rev. Lett.* **54**, 2611 (1985).

2. F. Bley, *Acta Metall. Mater.* **40**, 1505 (1992).

3. M. K. Miller *et al., Acta Metall. Mater.* **43**, 3385 (1995).

4. A. Mikikits-Leitner *et al., Phys. Rev. B* **82**, 100101 (2010).

5. H. Yamamoto, *Jap. J. Appl. Phys.* **3**, 745 (1964).

6. Z. Yan *et al., J. Alloys Compd.* **725**, 1035 (2017).

7. Y. Li, *J. Nucl. Mater.* **497**, 154 (2017).

8. W. Xiong *et al., Critical Reviews in Solid State and Materials Sciences* **35**, 125 (2010).

9. W. Xiong *et al., CALPHAD: Comput. Coupling Phase Diagrams Thermochem.* **35**, 355 (2011).

10. O. Senninger *et al., Acta Mater.* **73**, 97 (2014).

11. E. Martinez *et al., Phys. Rev. B* **86**, 224109 (2012).

12. M. Levesque *et al., Phys. Rev. B* **84**, 184205 (2011).

13. M. Yu. Lavrentiev, S. L. Dudarev, and D. Nguyen-Manh, *J. Nucl. Mater.* **386–388**, 22 (2009).

14. M. Yu. Lavrentiev, D. Nguyen-Manh, and S. L. Dudarev, *Phys. Rev. B* **81**, 184202 (2010).

15. M. Yu. Lavrentiev *et al., J. Phys.: Condens. Matter* **24**, 326001 (2012).

16. M. Yu. Lavrentiev *et al., Phys. Rev. B* **84**, 144203 (2011).

17. C.-C. Fu *et al., Phys. Rev. B* **91**, 094430 (2015).

18 J. Marro *et al., Phys. Rev. B* **12**, 2000 (1975).

19. R. Wagner, R. Kampmann, and P. W. Voorhees. Homogeneous Second-Phase Precipitation, in: Materials Science and Technology (eds R. W. Cahn, P. Haasen, and E. J. Kramer), 2013.

20. D. Nguyen-Manh, M. Yu. Lavrentiev, and S.L. Dudarev, *C.R. Phys.* **9**, 379 (2008).

21. M. Yu. Lavrentiev, D. Nguyen-Manh, and S. L. Dudarev, *Comp. Mat. Sci.* **49**, S199 (2010).

22. N. Castin *et al., J. Nucl. Mater.* **417**, 1086 (2011).

23. M. Furusaka *et al., J. Phys. Soc. Japan* 55, 2253 (1986).

24. E. Fawcett *et al., Rev. Mod. Phys.* **66**, 25 (1994).

25. S. K. Burke *et al., J. Phys. F* **13**, 451 (1983).

t = 0.8589 s   t= 350.44 s

t = 21019 s   t = 783396 s
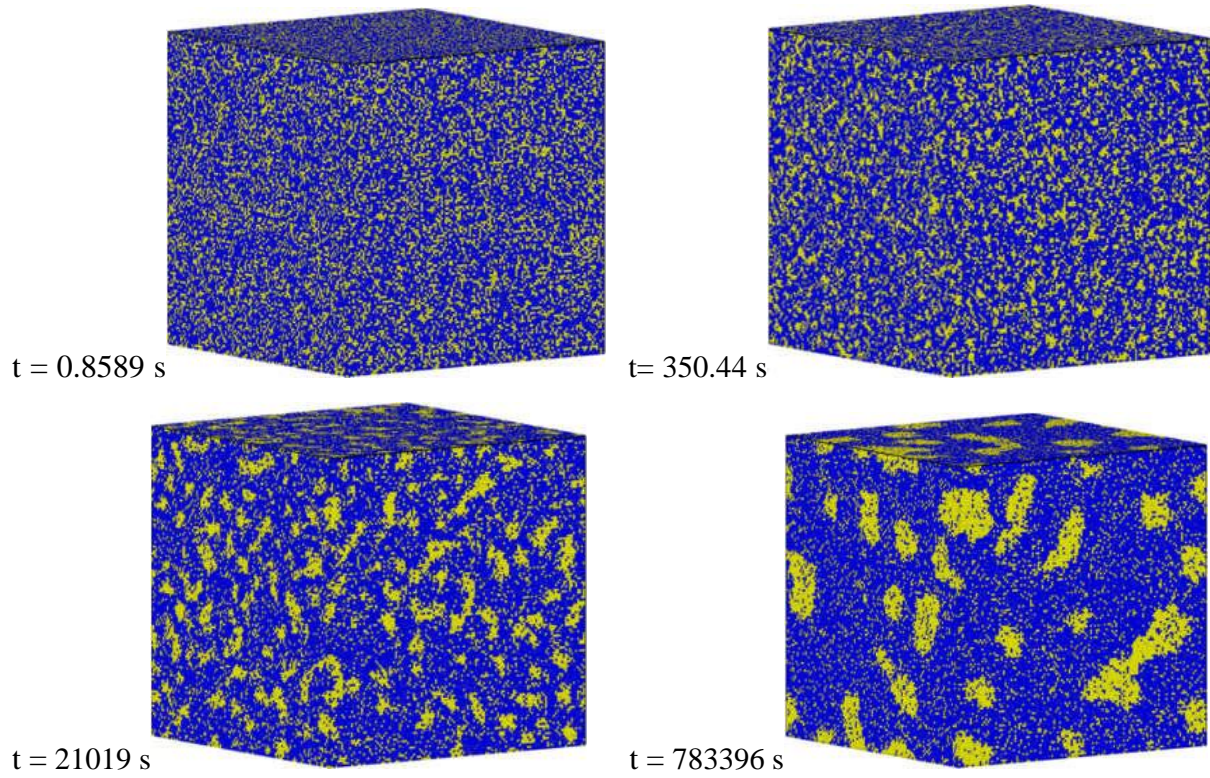
Figure 1. Time evolution of microstructure of Fe-32 at. % Cr alloy in kMC simulations. Blue colour – Fe atoms, yellow colour – Cr atoms.
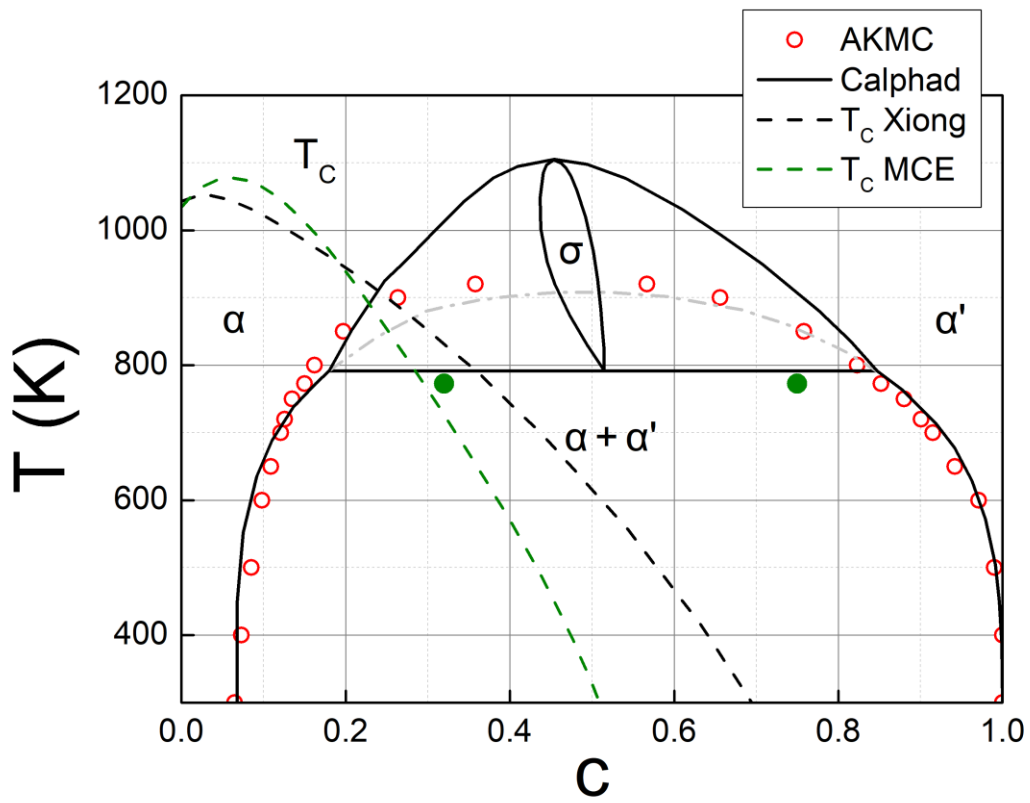
Figure 2. The Fe–Cr phase diagram. The green dots correspond to the alloys studied in this paper at temperature $T = 500°$ C.
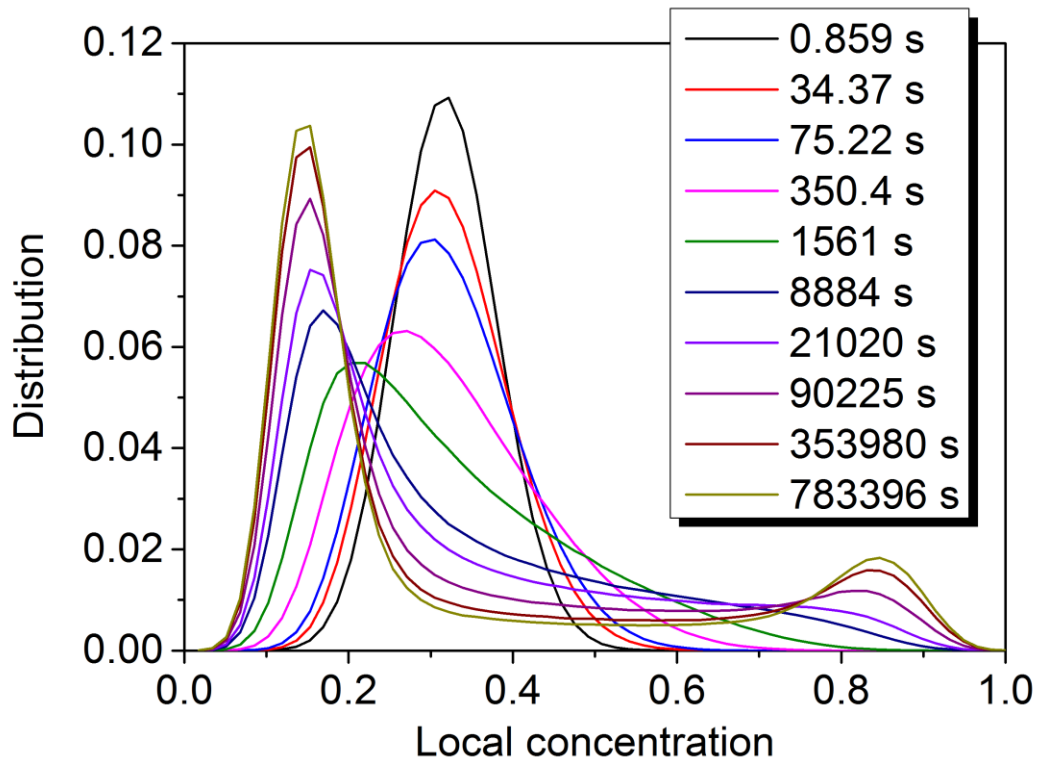
Figure 3. Distribution of local concentration in Cr clusters.
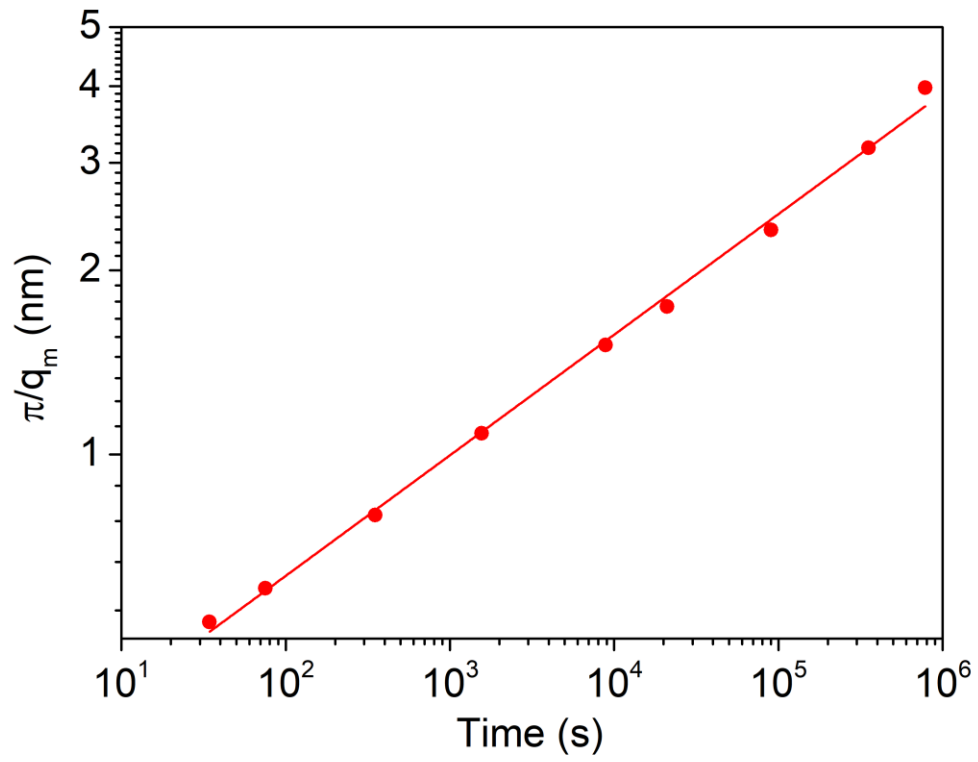
Figure 4. Time dependence of π/q_m in Fe-32 at. % Cr annealed at T = 500° C.
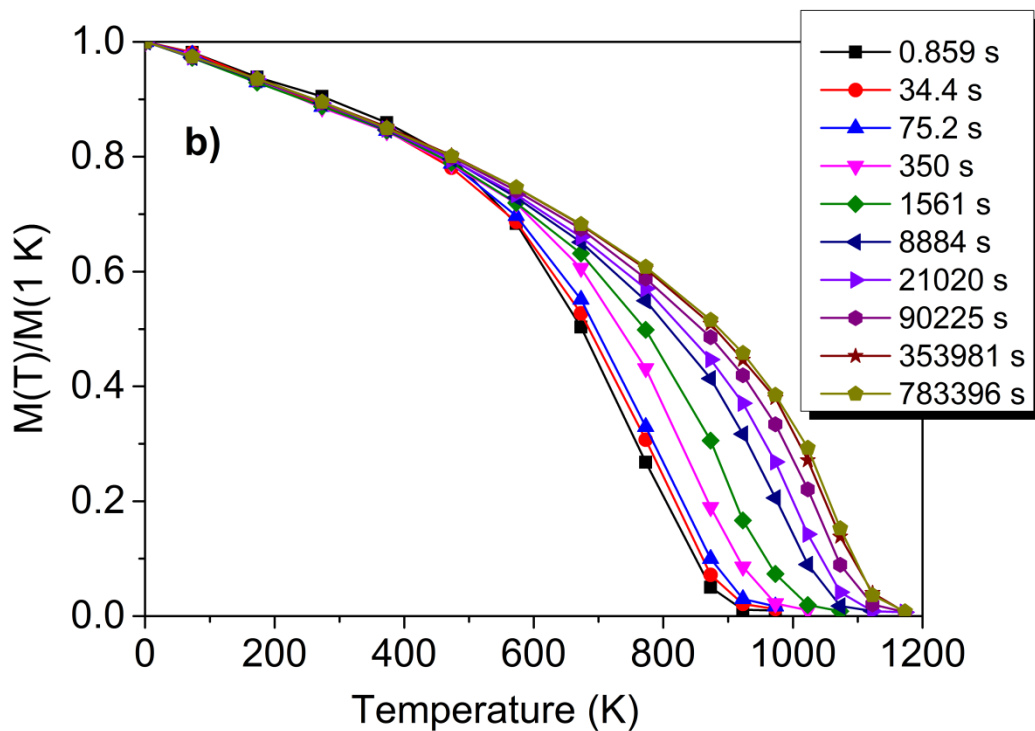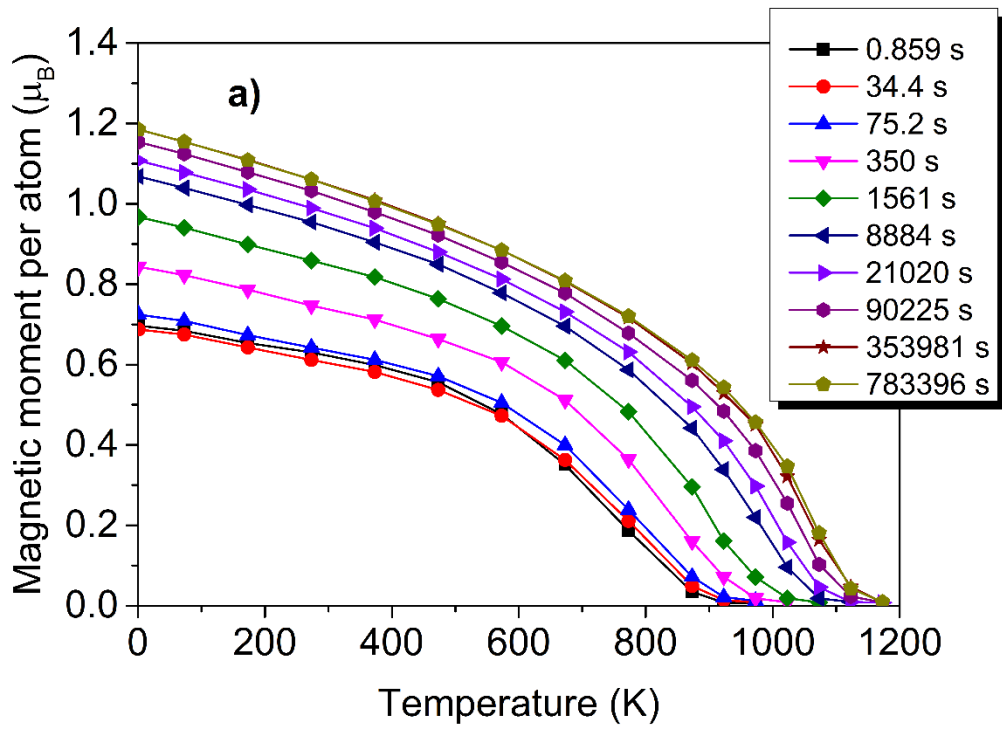
Figure 5. Magnetic moment *M(T)* per atom of Fe-32 at. % Cr system for configurations shown in Figure 1 (a) and *M(T)/M(1 K)* for the same configurations (b).
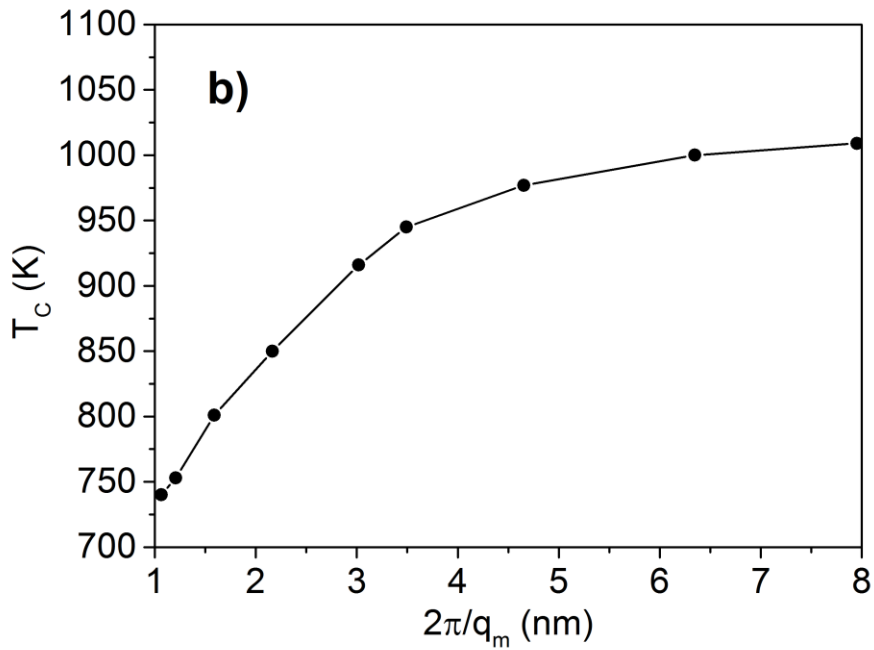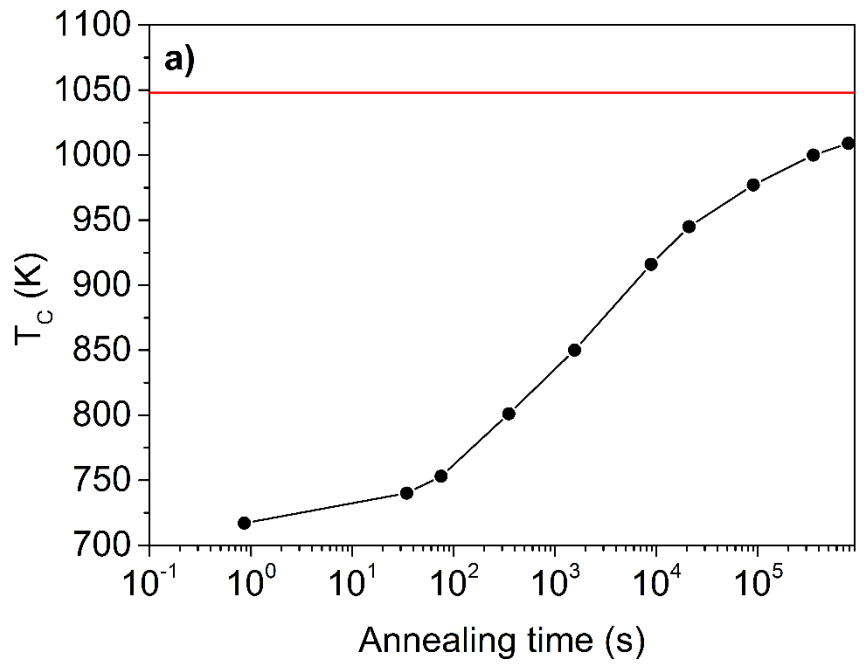
Figure 6. Curie temperature of Fe-32 at. % Cr alloy as a function of annealing time (a) and π/q_m (b). Red line in Figure 6a corresponds to the Curie temperature of Fe-15 at. % Cr (~1020 K in the current MCE simulation).

t = 3.363 s

t= 59133 s

t= 576935 s

t = 2275429 s
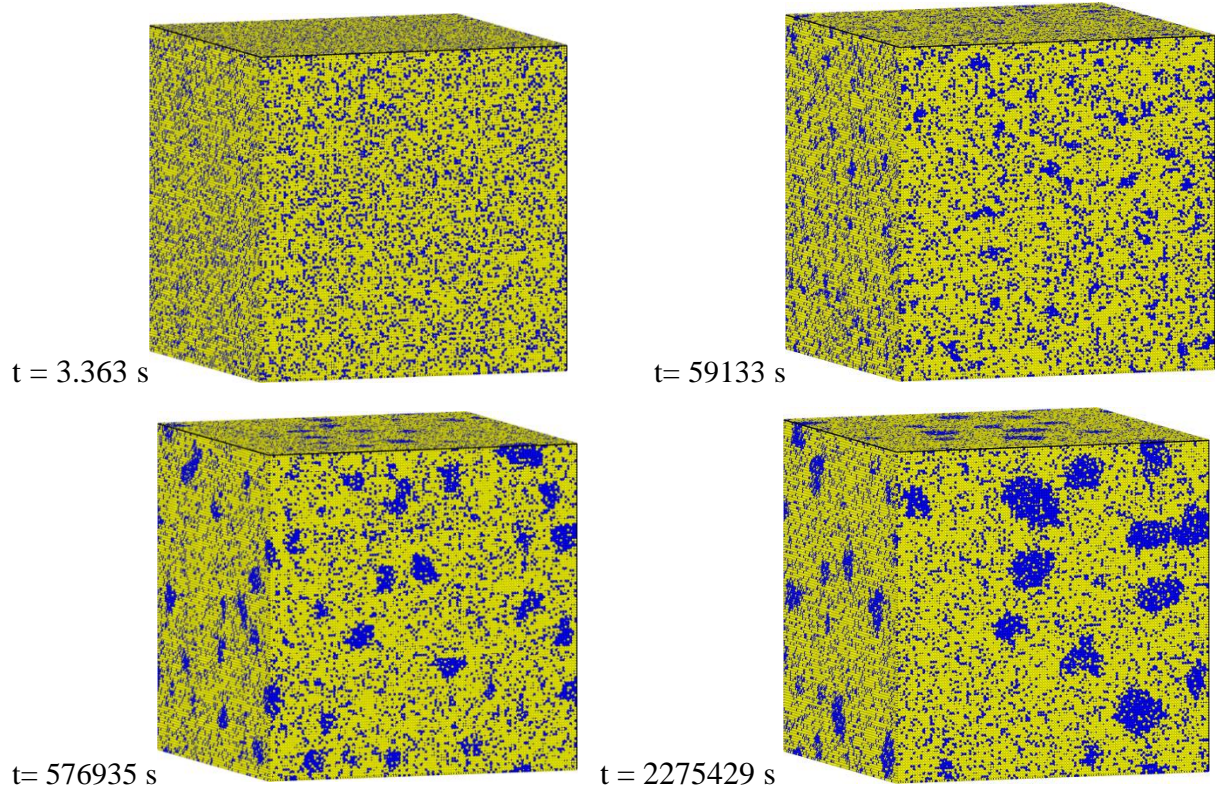
Figure 7. Time evolution of microstructure of Cr-25 at. % Fe alloy in kMC simulations. Blue colour – Fe atoms, yellow colour – Cr atoms.
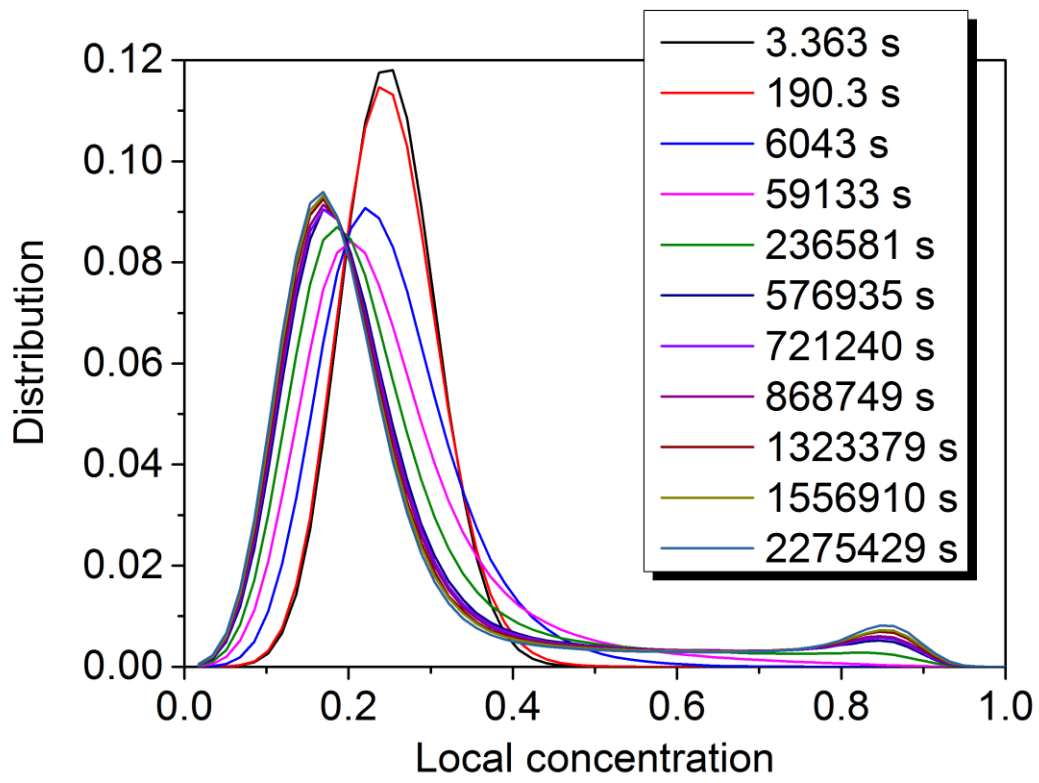
Figure 8. Distribution of local concentration in Fe clusters.
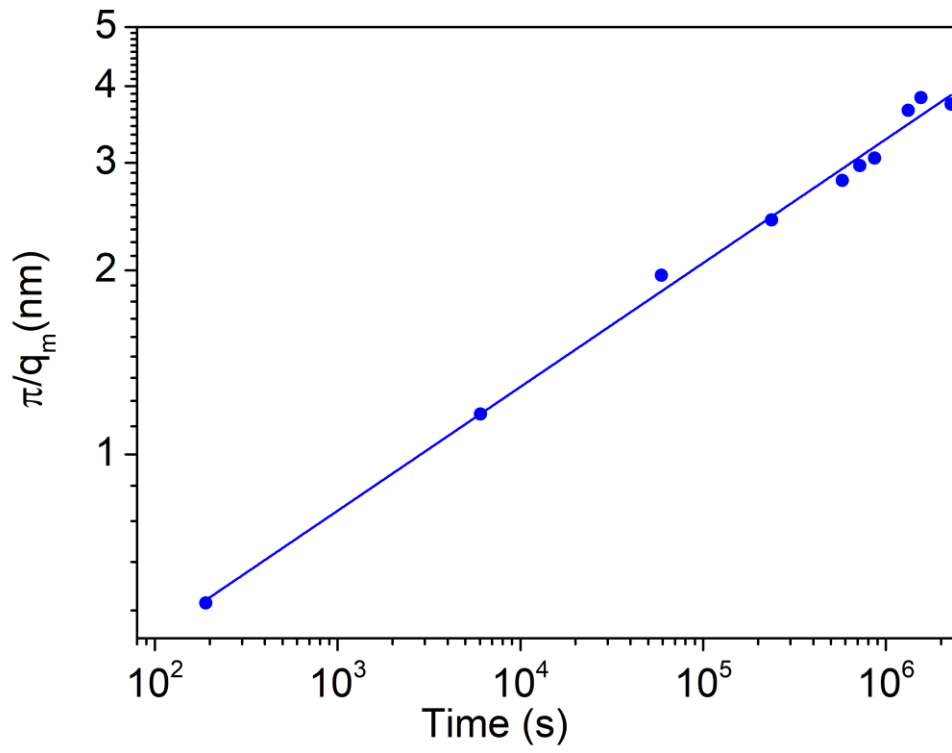
Figure 9. Time dependence of π/q_m in Cr-25 at. % Fe annealed at T = 500° C.
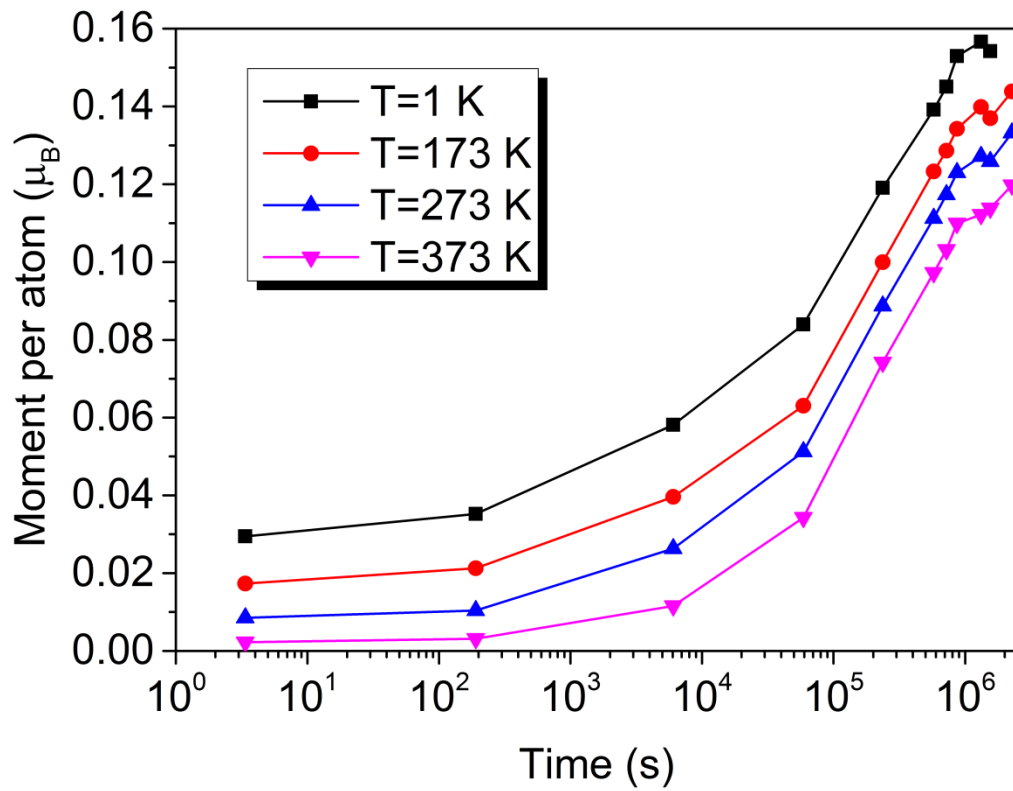
Figure 10. Magnetic moment of Cr-25 at. % Fe system as function of annealing time for temperatures between 1 K and 373 K.
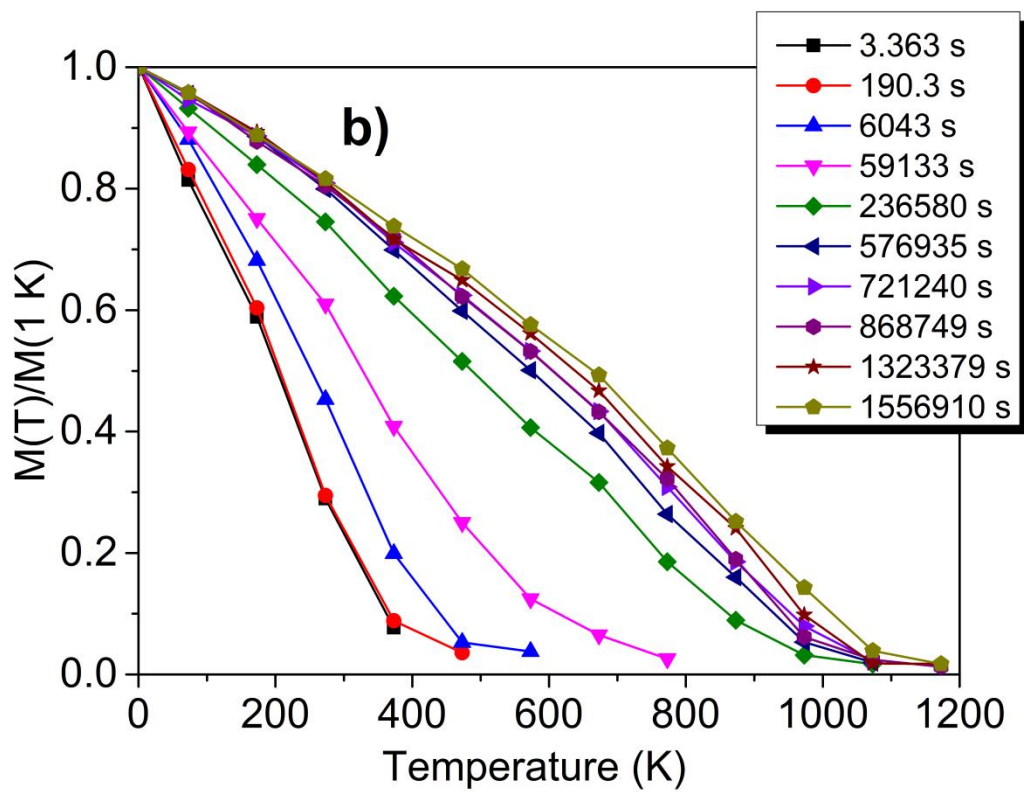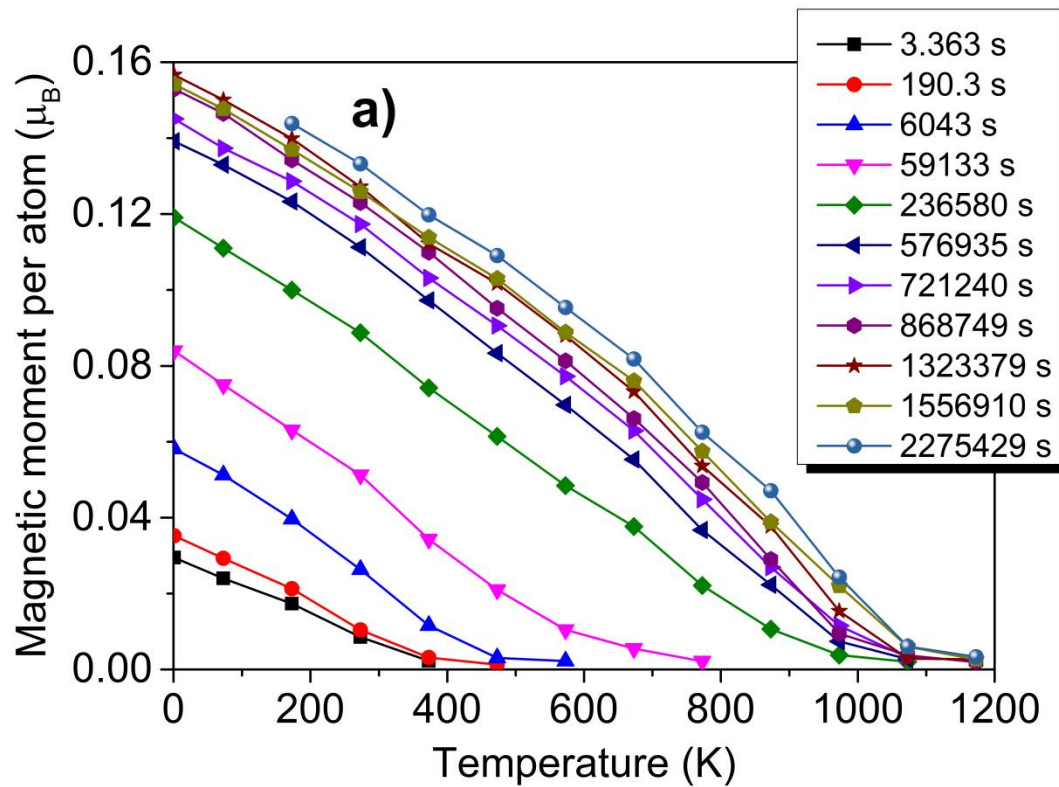
Figure 11. Magnetic moment *M(T)* per atom of Cr-25 at. % Fe system for configurations shown in Figure 7 (a) and *M(T)/M(1 K)* for the same configurations (b).
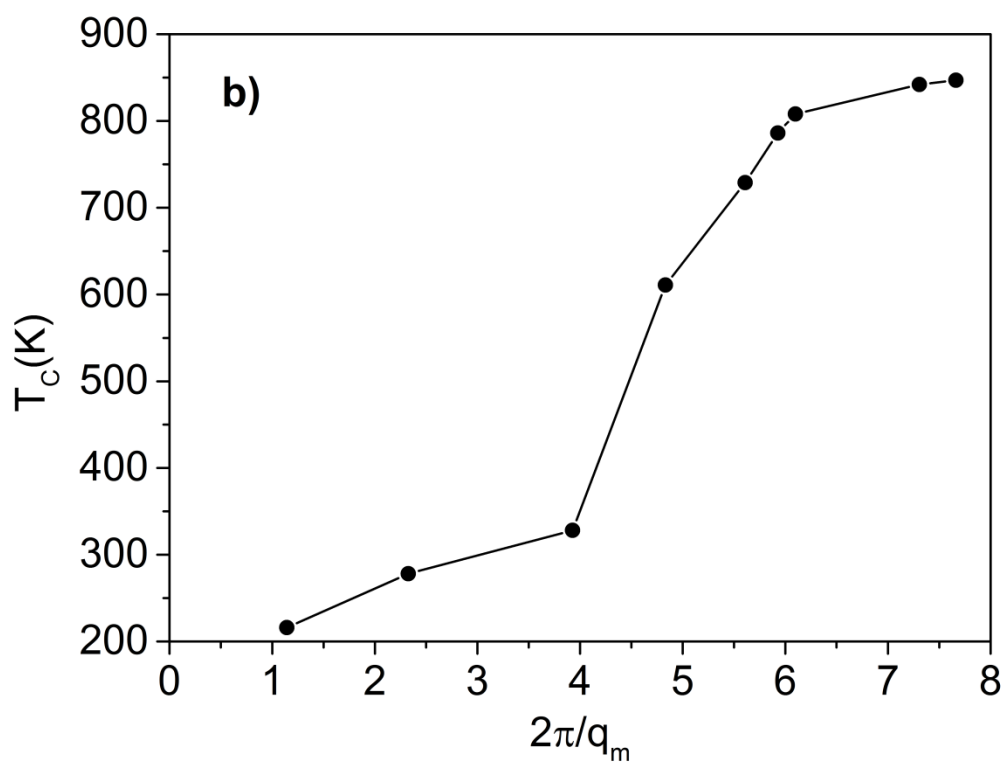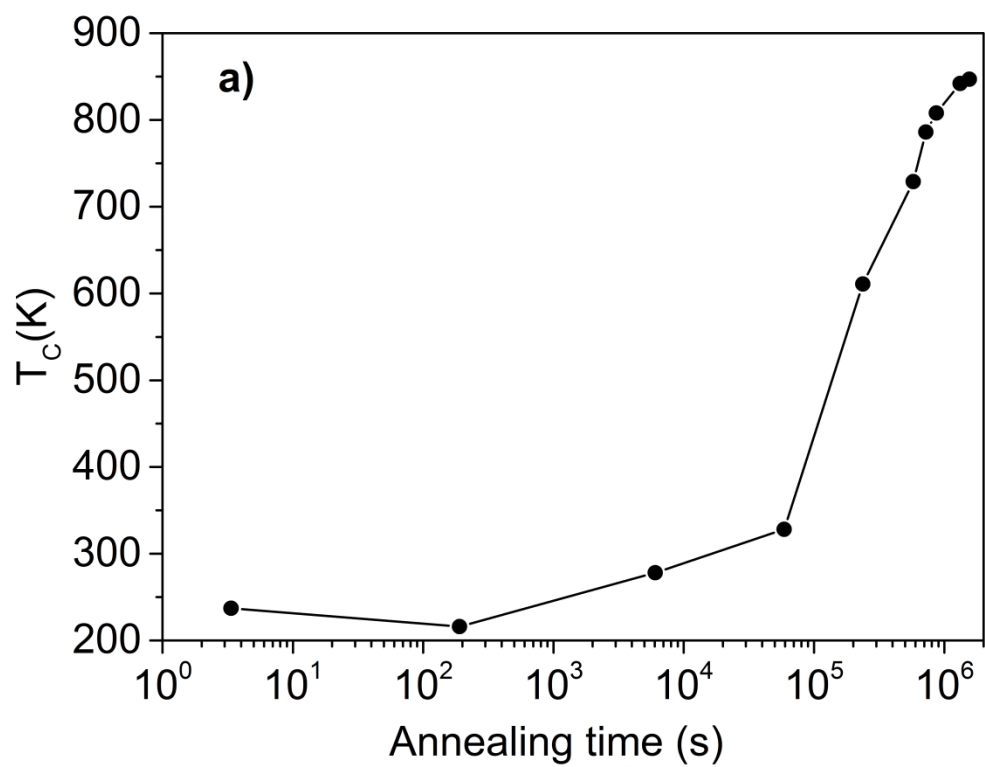
Figure 12. Curie temperature of Cr-25 at. % Fe alloy as a function of annealing time (a) and π/q_m (b).